

Free energy reconstruction from nonequilibrium single-molecule pulling experiments

Gerhard Hummer* and Attila Szabo

Laboratory of Chemical Physics, National Institute of Diabetes and Digestive and Kidney Diseases, National Institutes of Health, Bethesda, MD 20892-0520

Communicated by David Chandler, University of California, Berkeley, CA, January 22, 2001 (received for review November 28, 2000)

Laser tweezers and atomic force microscopes are increasingly used to probe the interactions and mechanical properties of individual molecules. Unfortunately, using such time-dependent perturbations to force rare molecular events also drives the system away from equilibrium. Nevertheless, we show how equilibrium free energy profiles can be extracted rigorously from repeated nonequilibrium force measurements on the basis of an extension of Jarzynski's remarkable identity between free energies and the irreversible work.

Recent advances in the micromanipulation of single molecules have led to new insights into the dynamics, interactions, structure, and mechanical properties of individual molecules (1–4). Single-molecule manipulation with an atomic force microscope (AFM) (5–9), laser tweezer stretching (10), and analogous computer experiments pioneered by Schulten and coworkers (11–13) have revealed details about unfolding and unbinding events of individual proteins and their complexes. In an AFM experiment, a molecule is subjected to a time-varying external force, for instance by pulling on the end of a linear polymer (Fig. 1). The applied force is determined from the time-dependent position of the cantilever tip with respect to the sample. Thus, one can drive rare molecular events (14), determine their force characteristics, and simultaneously monitor them with atomic resolution. However, both experiments and simulations actively perturb the system, leading to hysteresis and nonequilibrium effects.

How can one extract equilibrium properties from such measurements that drive the system away from equilibrium (15, 16)? From the second law of thermodynamics, we know that on average, the mechanical work of pulling will be larger than the free energy. Only if the experiment is performed reversibly, i.e., infinitely slowly, will the work equal the free energy. Thus, making rigorous thermodynamic measurements by pulling appears to require an extrapolation to zero pulling speed. However, Jarzynski (17, 18) recently discovered a remarkable *identity* between thermodynamic free energy differences and the irreversible work, thus extending the *inequality* of the second law of thermodynamics. This identity, although not directly applicable to atomic force measurements, suggests that in principle one should be able to extract free energy surfaces from *repeated* pulling experiments. In this paper, we show how this can be done in practice.

Theory. We begin by showing that Jarzynski's identity follows almost immediately from the Feynman–Kac theorem for path integrals (19). This derivation leads directly to the appropriate extension, which forms the basis for the solution of the free energy reconstruction problem. This extension has been obtained by Crooks (20) as a special case of an even more general relation between forward and backward path averages. Consider a system whose phase-space density evolves according to a Liouville-type equation:

$$\frac{\partial f(\mathbf{x}, t)}{\partial t} = \mathcal{L}_t f(\mathbf{x}, t). \quad [1]$$

\mathcal{L}_t is an explicitly time-dependent evolution operator that has the Boltzmann distribution as a stationary solution, $\mathcal{L}_t e^{-\beta \mathcal{H}(\mathbf{x}, t)} = 0$,

where $\mathcal{H}(\mathbf{x}, t)$ is a time-dependent Hamiltonian, and $\beta^{-1} = k_B T$, with T the temperature and k_B Boltzmann's constant. For example, for diffusive dynamics on a potential $V(\mathbf{x}, t)$, the time evolution is governed by $\mathcal{L}_t = D \nabla e^{-\beta V(\mathbf{x}, t)} \nabla e^{\beta V(\mathbf{x}, t)}$, where D is the diffusion coefficient and $\nabla = \partial/\partial \mathbf{x}$. Other examples include systems that undergo Newtonian, Langevin, Nosé–Hoover thermostat, or Metropolis Monte Carlo dynamics. Now consider the unnormalized Boltzmann distribution at time t ,

$$p(\mathbf{x}, t) = \frac{e^{-\beta \mathcal{H}(\mathbf{x}, t)}}{\int e^{-\beta \mathcal{H}(\mathbf{x}', 0)} d\mathbf{x}'}. \quad [2]$$

Because this distribution is stationary ($\mathcal{L}_t p = 0$), and because $\partial p/\partial t = -\beta(\partial \mathcal{H}/\partial t)p$, it follows that the above $p(\mathbf{x}, t)$ is a solution of the sink equation,

$$\frac{\partial p}{\partial t} = \mathcal{L}_t p - \beta \frac{\partial H}{\partial t} p, \quad [3]$$

as can be verified by direct substitution. However, the solution of this sink equation, starting from an equilibrium distribution at time $t = 0$, can also be expressed as a path integral by using the Feynman–Kac theorem (19). Equating these two different solutions immediately gives:

$$\frac{e^{-\beta \mathcal{H}(\mathbf{x}, t)}}{\int e^{-\beta \mathcal{H}(\mathbf{x}', 0)} d\mathbf{x}'} = \left\langle \delta(\mathbf{x} - \mathbf{x}_t) \exp \left[-\beta \int_0^t \frac{\partial \mathcal{H}}{\partial t'}(\mathbf{x}_{t'}, t') dt' \right] \right\rangle \quad [4]$$

where $\delta(\mathbf{x})$ is Dirac's δ distribution. This *identity* between a weighted average of nonequilibrium trajectories (right) and the equilibrium Boltzmann distribution (left) is implicit in the work of Jarzynski (18), and is given explicitly by Crooks (equation 24, ref. 20). The average $\langle \dots \rangle$ is over an ensemble of trajectories starting from the equilibrium distribution at $t = 0$ and evolving according to Eq. 1. Each trajectory is weighted with the Boltzmann factor of the external work w_t done on the system,

$$w_t = \int_0^t \frac{\partial \mathcal{H}}{\partial t'}(\mathbf{x}_{t'}, t') dt'. \quad [5]$$

Integrating both sides of Eq. 4 with respect to \mathbf{x} , we obtain Jarzynski's identity (17, 18)

Abbreviation: AFM, atomic force microscopy.

See commentary on page 3636.

*To whom reprint requests should be addressed at: LCP/NIDDK, Bldg. 5, Rm. 132, National Institutes of Health, Bethesda, MD 20892-0520. E-mail: hummer@helix.nih.gov.

The publication costs of this article were defrayed in part by page charge payment. This article must therefore be hereby marked "advertisement" in accordance with 18 U.S.C. §1734 solely to indicate this fact.

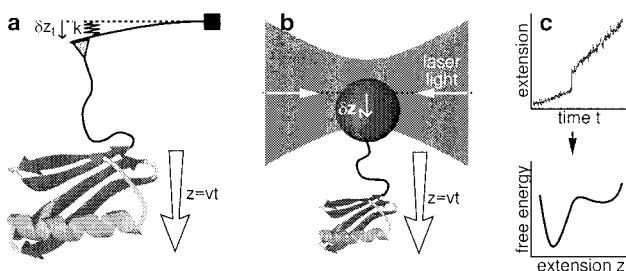


Fig. 1. Single-molecule force measuring experiments by using AFM (a) and laser tweezers (b). In the AFM experiment (a), the sample is moved at a constant speed v relative to the cantilever with spring constant k . The position $z_t = vt + \delta z_t$ of the cantilever tip with respect to the sample is recorded, where δz_t is the displacement of the cantilever tip. From repeated measurements of z_t , the free energy profile $G_0(z)$ of the unperturbed system can be determined exactly (c).

$$e^{-\beta \Delta G(t)} \equiv \frac{\int e^{-\beta \mathcal{H}(\mathbf{x}, t)} d\mathbf{x}}{\int e^{-\beta \mathcal{H}(\mathbf{x}, 0)} d\mathbf{x}} = \langle e^{-\beta w_t} \rangle, \quad [6]$$

between the Boltzmann-averaged work w_t and the equilibrium free energy difference $\Delta G(t)$ between times t and 0.

Free Energy Surfaces from Cantilever Positions. Eq. 4 allows us to reconstruct the underlying free energy surface from repeated single-molecule AFM experiments. The setup in Fig. 1a can be described by a Hamiltonian $\mathcal{H}(\mathbf{x}, t) = \mathcal{H}_0(\mathbf{x}) + k(z - vt)^2/2$, where $\mathcal{H}_0(\mathbf{x})$ is the Hamiltonian of the resting, unperturbed system, and $z = z(\mathbf{x})$. Here, we have assumed for simplicity that the cantilever is vibrating in a harmonic potential with spring constant k . Substituting this Hamiltonian into Eq. 4, multiplying both sides by $\delta[z - z(\mathbf{x})]$, integrating over all \mathbf{x} , and finally taking the logarithm, we have:

$$G_0(z) \equiv -\beta^{-1} \ln \frac{\int \delta[z - z(\mathbf{x})] e^{-\beta \mathcal{H}_0(\mathbf{x})} d\mathbf{x}}{\int e^{-\beta \mathcal{H}_0(\mathbf{x}, 0)} d\mathbf{x}} = -\beta^{-1} \ln \langle \delta(z - z_t) e^{-\beta \Delta w_t} \rangle, \quad [7]$$

where $G_0(z)$ is (to within an additive constant) the unperturbed free energy profile along the pulling coordinate z ; and Δw_t is the external work minus the instantaneous biasing potential, $\Delta w_t = w_t - k(z_t - vt)^2/2 = kv(vt^2/2 - \int_0^t z_t' dt') - k(z_t - vt)^2/2$. At time $t = 0$, the trajectories are started from points z_0 drawn from a Boltzmann distribution corresponding to Hamiltonian $\mathcal{H}(\mathbf{x}, 0) = \mathcal{H}_0(\mathbf{x}) + kz^2/2$.

Given the positions z_t of the cantilever at time t obtained from repeated pulling experiments, we can reconstruct the unperturbed free energy profile $G_0(z)$ along z by using Eq. 7. At each time slice t , one can in principle obtain an estimate of the whole free energy surface. In practice, at any given time t , only a small window around the equilibrium position $z = vt$ will be sampled adequately. Thus, an average over several time slices and repeated trajectories is required to obtain an optimal estimate of the free energy surface. At every time slice t , one obtains an ensemble of positions z_t and corresponding w_t s. The positions z_t are binned, and the corresponding histogram values are incremented by $e^{-\beta w_t}$. The complete free energy surface $G_0(z)$ can

then be reconstructed by adapting the weighted histogram method (21):

$$G_0(z) = -\beta^{-1} \ln \frac{\sum_t \langle \delta(z - z_t) \exp(-\beta w_t) \rangle}{\sum_t \frac{\exp[-\beta u(z, t)]}{\langle \exp(-\beta w_t) \rangle}}, \quad [8]$$

where the sum is over time slices t and $u(z, t)$ is the time-dependent biasing potential [here: $u(z, t) = k(z - vt)^2/2$]. As in the weighted histogram method (21), this procedure can be refined by making Eq. 8 self-consistent through replacement of $\langle \exp(-\beta w_t) \rangle$ with $\exp[-\beta \Delta G(t)] = \int \exp\{-\beta[u(z, t) + G_0(z)]\} dz / \int \exp\{-\beta[u(z, 0) + G_0(z)]\} dz$, thus requiring an iterative solution for $\Delta G(t)$.

To illustrate in detail how this formalism is implemented, we simulate a pulling experiment by conducting Brownian-dynamics simulations on a double-well free energy surface. Ten trajectories were generated on the time-dependent surface $V(z) + k(z - vt)^2/2$ with a pulling velocity $v = 1 \mu\text{m s}^{-1}$, a diffusion coefficient $D = 10^{-7} \text{cm}^2 \text{s}^{-1}$, and a cantilever spring constant $k = 20.6 \text{pN nm}^{-1}$ ($=0.0206 \text{mN m}^{-1}$). The pulling velocities and cantilever spring constants are typical of AFM experiments (2, 6). For this diffusion coefficient, the escape rate from the stable minimum is about 10^{-6}s^{-1} on the basis of Kramers' theory, in the range of unfolding rates for fairly large proteins under native conditions. The free energy difference between the two states separated by a barrier is $\approx 14 \text{kcal/mol}$ (at 298 K), again typical of protein unfolding. Nevertheless, this simple one-dimensional model is only a crude approximation to real experiments where several other factors intrude, such as viscous damping of the cantilever motion or slow conformational relaxation orthogonal to the pulling direction (14).

In the pulling simulations, the ‘‘cantilever’’ is moved relative to the ‘‘sample’’ by 20 nm within a time of 20 ms. The position z_t and accumulated work $w_t = kv(vt^2/2 - \int_0^t z_t' dt')$ are recorded for 10 runs and analyzed by using Eq. 7. For every pulling trajectory k ($k = 1, \dots, K$; here: $K = 10$), we determine at discrete times t_i ($i = 0, \dots, N$; here: $N = 100$ time points separated by 0.2 ms) the position of the cantilever z_{ik} with respect to the sample, and the corresponding deflection $\delta z_{ik} = z_{ik} - vt_i$. From the deflection, we obtain the instantaneous deflection energy $u_{ik} = k\delta z_{ik}^2/2$. The external work is determined by numerical integration: $w_{ik} = kv[v t_i^2/2 - \sum_{j=1}^i (t_j - t_{j-1})(z_{jk} + z_{j-1,k})/2]$ with $w_{ik} = 0$ for $i = 0$. The results of repeated trajectories are then combined. At every time slice t_i , we average $\langle \exp(-\beta w_t) \rangle \approx \eta_i \equiv K^{-1} \sum_{k=1}^K \exp(-\beta w_{ik})$. To approximate the average in the top numerator of Eq. 8, we also collect histograms $h_i(l)$ at times t_i with z -position intervals of Δz :

$$h_i(l) = K^{-1} \sum_{k=1}^K e^{-\beta w_{ik}} \theta_l(z_{ik}), \quad [9]$$

where $\theta_l(z)$ is one if z is in the l th interval [$(l - 1)\Delta z \leq z < l\Delta z$] and zero otherwise. We then estimate the free energy profile by averaging over all time slices t_i :

$$G_0[(l - 1/2)\Delta z] = -\beta^{-1} \ln \frac{\sum_{i=0}^N h_i(l)/\eta_i}{\sum_{i=0}^N \exp(-\beta u_{ik})/\eta_i}. \quad [10]$$

Fig. 2 compares the reconstructed and exact free energy surfaces. With the exception of the poorly sampled barrier region because of snapping motion (Fig. 2 Inset), the surface is accurately reproduced. We note that at high pulling speeds, the

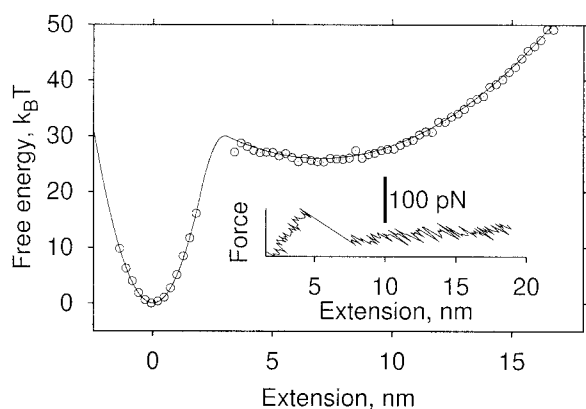


Fig. 2. Simulated pulling experiment over a $30 k_B T$ barrier. The solid line and symbols show the reference free energy $V(z)$ and the reconstruction from 10 pulling simulations, respectively. *Inset* shows the force-versus-extension curve for one of the pulling simulations.

increasing variance of w_i will lead to a systematic bias of the estimator for $-\beta^{-1} \ln \langle \delta(z - z_i) \exp(-\beta w_i) \rangle$, which can be approximately corrected for by using a cumulant expansion.

Free Energy Surfaces from Pulling Forces. So far, we made use of position-versus-time curves. However, it is force-versus-position curves that are commonly reported from pulling experiments. As above, we assume a Hamiltonian $\mathcal{H}(\mathbf{x}, t) = \mathcal{H}_0(\mathbf{x}) + u[z(\mathbf{x}), t]$. The unperturbed system described by \mathcal{H}_0 is coupled to the measurement apparatus through $u[z(\mathbf{x}), t]$, which will typically be a harmonic potential, $u[z(\mathbf{x}), t] = k(z - vt)^2/2$. The work entering the free energy expression Eq. 9 can be rewritten as

$$\Delta w_i \equiv w_i - u(z_i, t) = \int_c F(z, t) dz - u(z_0, 0), \quad [11]$$

where the restoring force is $F(z, t) = -\partial u(z, t)/\partial z$, and the integral is along the position-versus-time contour connecting z_0 and z_i . This identity follows from $du = (\partial u/\partial z) dz + (\partial u/\partial t) dt$. Combining Eqs. 7 and 11 leads to the surprising result that the work entering into the free energy profile $G_0(z)$ is *not* given simply by the force-versus-distance integral, but by an additional factor reflecting the biased choice of the initial state,

$$G_0(z) = -\beta^{-1} \ln \langle \delta(z - z_i) e^{-\beta [\int_c F(z, t) dz - u(z_0, 0)]} \rangle, \quad [12]$$

where the initial points are drawn from a Boltzmann distribution according to $\mathcal{H}(\mathbf{x}, 0)$ (i.e., for the system interacting with the cantilever, as above). Therefore, if force integrals of two or more trajectories are combined, individual trajectories should be weighted by the reciprocal Boltzmann factor $\exp[\beta u(z_0, 0)]$; i.e., one should subtract from the integrated work the energy stored in the deflected cantilever at time $t = 0$.

In an AFM experiment, it is thus important to record the zero-force position ($\delta z = 0$ in Fig. 1) with the cantilever sufficiently far from the sample. As the cantilever tip is brought into contact with the sample, a sufficiently long relaxation is important to draw initial states from an equilibrium Boltzmann distribution. We note that this new equilibrium will normally not be centered around $\delta z = 0$, but according to the combined Hamiltonian $\mathcal{H}(\mathbf{x}, 0)$ of the sample coupled to the cantilever spring. Nevertheless, the center of this initial distribution can be used to align the z positions of repeated pulling traces. As the cantilever is retracted, both z_i and δz_i are recorded. With known cantilever spring constant k and pulling speed v , the work can then be obtained from time or position integration.

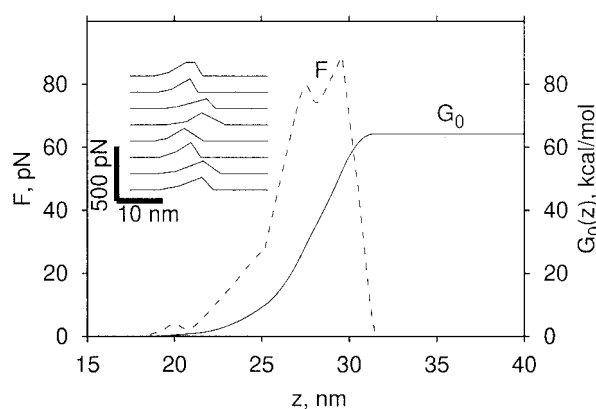


Fig. 3. Free energy $G_0(z)$ (solid line, right-hand scale) and mean restoring force $F(z) = dG_0(z)/dz$ (dashed line, left-hand scale) of extracting and unfolding the D and E helix of the G241C mutant of bacteriorhodopsin. Eq. 12 was used to estimate $G_0(z)$ from linear approximations (*Inset*) to the second peak of eight force-versus-distance curves reported in figure 5, Oesterhelt *et al.* (8).

As a final illustration, we analyze force spectra for extracting individual bacteriorhodopsin molecules from purple membrane patches of *Halobacterium salinarum* as measured by Oesterhelt *et al.* (8). In these experiments, a cantilever tip was attached to bacteriorhodopsin, and the protein was slowly pulled out of the membrane. This led to sequential unraveling of the transmembrane helices, resulting in unfolding of the protein. Specifically, we analyze the force-versus-distance curves for one of the experiments (G241C mutant) and estimate a free energy profile for extraction and unfolding of helices D and E, corresponding to the second peak at pulling distances of 20–30 nm in figure 5 of ref. 8. Because the force is fluctuating around the baseline before and after this force peak, we assume (i) that the additional bias $u(z_0, 0)$ in Eq. 12 is of the order of $k_B T$ and thus negligible on the scale of the integrated work; and that (ii) a quasiequilibrium was established before the force peak. We also assume (iii) that the force curves are aligned. We can then integrate the forces and use Eq. 12 to estimate the underlying free energy profile $G_0(z)$, as shown in Fig. 3. Also shown is the mean restoring force, $F(z) = dG_0(z)/dz$, corresponding to reversible pulling. The noise in the force $F(z)$ reflects uncertainties in the z -position alignment and the finite number of measurements. For extraction and stretching of the 57-amino acid stretch with 56 amino acids contained in helices D and E, we estimate a free energy of about 64 kcal/mol, or about 1.1 kcal/mol per residue, and a mean-force peak of about 89 pN. Although these values seem overall reasonable, they should not be considered to be accurate before the above assumptions are removed by appropriate experimental design. In addition, one must account for instrument resolution, which leads to increased variation of the integrated work. Finally, the influence of the pulling speed needs to be investigated. In general, to extract accurate thermodynamic information from a small number of pulling experiments, it will be important to achieve small standard deviations of the work, possibly of a few $k_B T$, by pulling sufficiently slowly.

Conclusions

We have shown how free energy surfaces can be reconstructed rigorously from repeated molecular pulling experiments. With this formalism, thermodynamic properties such as binding equilibria can be extracted from repeated measurements by using AFM (2, 5–9, 12), laser tweezers (1, 4), or magnetic beads (3). In addition, this work has implications in the area of computer simulations. For example, when a time-dependent harmonic

potential is added to the Hamiltonian as above, our procedure is a dynamic generalization of umbrella sampling (22). The weighted-histogram method permits the combination of dynamic umbrella sampling runs with different pulling speeds or

directions. Moreover, this generalization has the immediate advantage that no equilibration is required in different windows, and thus the entire trajectory can be used to reconstruct the underlying free energy surface.

1. Perkins, T. T., Smith, D. E. & Chu, S. (1994) *Science* **264**, 819–822.
2. Florin, E. L., Moy, V. T. & Gaub, H. E. (1994) *Science* **264**, 415–417.
3. Strick, T. R., Allemand, J. F., Bensimon, D., Bensimon, A. & Croquette, V. (1996) *Science* **271**, 1835–1837.
4. Smith, S. B., Cui, Y. J. & Bustamante, C. (1996) *Science* **271**, 795–799.
5. Tskhovrebova, L., Trinick, J., Sleep, J. A. & Simmons, R. M. (1997) *Nature (London)* **387**, 308–312.
6. Rief, M., Gautel, M., Oesterhelt, F., Fernandez, J. M. & Gaub, H. E. (1997) *Science* **276**, 1109–1112.
7. Oberhauser, A. F., Marszalek, P. E., Erickson, H. P. & Fernandez, J. M. (1998) *Nature (London)* **393**, 181–185.
8. Oesterhelt, F., Oesterhelt, D., Pfeiffer, M., Engel, A., Gaub, H. E. & Müller, D. J. (2000) *Science* **288**, 143–146.
9. Merkel, R., Nassoy, P., Leung, A., Ritchie, K. & Evans, E. (1999) *Nature (London)* **397**, 50–53.
10. Keller Mayer, M. S. Z., Smith, S. B., Granzier, H. L. & Bustamante, C. (1997) *Science* **276**, 1112–1116.
11. Isralewitz, B., Izrailev, S. & Schulten, K. (1997) *Biophys. J.* **73**, 2972–2979.
12. Marszalek, P. E., Lu, H., Li, H. B., Carrion-Vazquez, M., Oberhauser, A. F., Schulten, K. & Fernandez, J. M. (1999) *Nature (London)* **402**, 100–103.
13. Paci, E. & Karplus, M. (1999) *J. Mol. Biol.* **288**, 441–459.
14. Dellago, C., Bolhuis, P. G., Csajka, F. S. & Chandler, D. (1998) *J. Chem. Phys.* **108**, 1964–1977.
15. Balsera, M., Stepaniants, S., Izrailev, S., Oono, Y. & Schulten, K. (1997) *Biophys. J.* **73**, 1281–1287.
16. Gullingsrud, J. R., Braun, R. & Schulten, K. (1999) *J. Comp. Phys.* **151**, 190–211.
17. Jarzynski, C. (1997) *Phys. Rev. Lett.* **78**, 2690–2693.
18. Jarzynski, C. (1997) *Phys. Rev. E* **56**, 5018–5035.
19. Schuss, Z. (1980) *Theory and Applications of Stochastic Differential Equations* (Wiley, New York).
20. Crooks, G. E. (2000) *Phys. Rev. E* **61**, 2361–2366.
21. Ferrenberg, A. M. & Swendsen, R. H. (1989) *Phys. Rev. Lett.* **63**, 1195–1198.
22. Torrie, G. M. & Valleau, J. P. (1974) *Chem. Phys. Lett.* **28**, 578–581.